

- (8) S. O. Grim, R. L. Keiter, and W. McFarlane, *Inorg. Chem.*, **6**, 1133 (1967).
 (9) F. H. Allen and S. N. Sze, *J. Chem. Soc. A*, 2054 (1971).
 (10) A. Pidcock, R. E. Richards, and L. M. Venanzi, *J. Chem. Soc. A*, 1707 (1966).
 (11) B. T. Heaton and A. Pidcock, *J. Organomet. Chem.*, **14**, 235 (1968).
 (12) W. E. Moddeman, J. R. Blackburn, G. Kumar, K. A. Morgan, R. G. Albridge, and M. M. Jones, *Inorg. Chem.*, **11**, 1715 (1972).
 (13) D. T. Clark, D. B. Adams, and D. Briggs, *Chem. Commun.*, 602 (1971).
 (14) C. D. Cook, K. Y. Wan, U. Gelius, K. Hamrin, G. Johansson, E. Olsson, H. Siegbahn, C. Nordling, and K. Siebahn, *J. Am. Chem. Soc.*, **93**, 1904 (1971).
 (15) D. P. Murtha and R. A. Walton, *Inorg. Chem.*, **12**, 368 (1973).
 (16) W. L. Jolly, *Coord. Chem. Rev.*, **13**, 47 (1974).
 (17) D. G. Tisley and R. A. Walton, *J. Inorg. Nucl. Chem.*, **35**, 1905 (1973).
 (18) S. Hagström, C. Nordling, and K. Siegbahn, *Z. Phys.*, **178**, 439 (1964).
 (19) M. M. Millard and G. Urry, *Inorg. Chem.*, **14**, 1982 (1975).
 (20) B. R. McGarvey, *J. Chem. Phys.*, **38**, 388 (1963).
 (21) E. Y. Wong, *J. Chem. Phys.*, **32**, 598 (1960).
 (22) G. F. Dionne, *Can. J. Phys.*, **42**, 2419 (1964).
 (23) G. Natta, P. Corradini, and G. Allegra, *J. Polym. Sci.*, **51**, 399 (1961).
 (24) P. C. Crouch, G. W. A. Fowles, and R. A. Walton, *J. Chem. Soc. A*, 972 (1969).
 (25) R. J. H. Clark, "The Chemistry of Titanium and Vanadium", Elsevier, Amsterdam 1968, p 178.
 (26) J. Lewis, D. J. Machin, I. E. Newnham, and R. S. Nyholm, *J. Chem. Soc.*, 2036 (1962).
 (27) R. J. H. Clark, "The Chemistry of Titanium and Vanadium", Elsevier, Amsterdam, 1968, pp 49, 179.
 (28) G. W. A. Fowles and B. J. Russ, *J. Chem. Soc. A*, 517 (1967).
 (29) R. J. H. Clark, *J. Chem. Soc.*, 417 (1964).
 (30) C. Dijkgraaf and J. P. G. Rousseau, *Spectrochim. Acta, Part A*, **23a**, 1267 (1967).
 (31) C. Dijkgraaf, *Nature (London)*, **201**, 1121 (1964).
 (32) D. M. Adams and P. J. Chandler, *J. Chem. Soc. A*, 588 (1969).
 (33) J. Goubeau and G. Wenzel, *Z. Phys. Chem.*, **45**, 31 (1965).
 (34) K. Shobatake, C. Postmus, J. R. Ferraro, and K. Nakamoto, *Appl. Spectrosc.*, **23**, 12 (1969).
 (35) K. Shobatake and K. Nakamoto, *J. Am. Chem. Soc.*, **92**, 3332 (1970).
 (36) S. H. Mastin, *Inorg. Chem.*, **13**, 1003 (1974).
 (37) G. S. Kyker, Ph.D. Dissertation, The Ohio State University, 1969, p 97.
 (38) H. C. Clark, K. R. Dixon, and W. J. Jacobs, *J. Am. Chem. Soc.*, **90**, 2259 (1968).
 (39) J. A. Creighton and J. H. S. Green, *J. Chem. Soc. A*, 808 (1968).
 (40) J. R. Ebner and R. A. Walton, *Inorg. Chem.*, **14**, 2289 (1975).
 (41) R. H. Lee, E. Griswold, and J. Kleinberg, *Inorg. Chem.*, **3**, 1278 (1964).

Contribution from the Chemical Engineering Division,
Argonne National Laboratory, Argonne, Illinois 60439

Spectrophotometric Study of the Cobalt(II) Bromide-Aluminum Bromide Vapor Complex

G. N. PAPTHeODOROU* and G. H. KUCERA

Received October 23, 1976

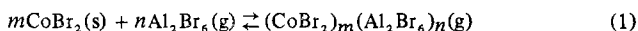
AIC60767+

The reaction of solid cobalt(II) bromide with gaseous aluminum bromide to form deep green gaseous complex(es) has been investigated spectrophotometrically in the range 550–900 K and at pressures up to 2 atm. Thermodynamic considerations suggest the reaction $\text{CoBr}_2(\text{s}) + \text{Al}_2\text{Br}_6(\text{g}) \rightleftharpoons \text{CoAl}_2\text{Br}_6(\text{g})$ [$\Delta H = 9.9$ kcal/mol; $\Delta S = 9.4$ eu]. The electronic absorption spectra are discussed in terms of the possible coordination of Co(II) in the gaseous molecule(s). Spectroscopic and thermodynamic considerations suggest that the predominant absorbing species in the gas phase is $\text{Co}(\text{AlBr}_4)_2$ molecules having the Co(II) in a close-to-octahedral coordination. The volatility enhancement ratios of cobalt(II) halide in the presence of various "acidic" A_2X_6 gases are calculated and compared. At temperatures below 750 K, aluminum bromide is a better gas-complexing agent than aluminum chloride for the respective cobalt halides.

Introduction

Recent spectrophotometric studies have established the thermodynamics and stoichiometry of the gaseous complexes formed on reacting aluminum chloride with transition metal halides [MCl_x : $\text{M} = \text{Pd}(\text{II})$,¹ $\text{Pt}(\text{II})$,² $\text{Co}(\text{II})$,^{3,4} $\text{V}(\text{II})$ and $\text{V}(\text{III})$,⁵ $\text{Cr}(\text{II})$,⁶ $\text{U}(\text{III})$ and $\text{U}(\text{IV})$,⁷ $\text{Nd}(\text{III})$].⁸ For the divalent transition metal chlorides the predominant gaseous species were found to be MAl_2Cl_6 .^{1-4,6} Furthermore, since the absorption spectra of these complexes are ligand field sensitive, some information about the structure of the gaseous molecule has been obtained. The electronic absorption spectra of $\text{Pt}(\text{II})$ and $\text{Pd}(\text{II})$ complexes were found to be compatible with a square-planar configuration of the "central"^{1,2} ion whereas for the $\text{Co}(\text{II})$ complex both octahedrally and tetrahedrally coordinated $\text{Co}(\text{II})$ atoms were considered.³ The spectra of $\text{V}(\text{II})$ ⁵ and $\text{Cr}(\text{II})$ ⁶ complexes were interpreted as having the transition metals in distorted octahedral chloride coordination.

In the present work, we report spectroscopic and thermodynamic data for the formation of the deep green gaseous complex(es) of aluminum bromide with cobalt bromide



The data are discussed in terms of the stoichiometry and possible structure of the gaseous complex and are compared with the corresponding data of the chloroaluminate complex(es) of $\text{Co}(\text{II})$.³

The purpose of this study is to examine the ability of aluminum bromide to form gaseous complexes and to compare the thermodynamics, structure, and volatility enhancement

ratios of the bromoaluminate complexes with those of the chloroaluminate complexes.

Experimental Section

High-purity anhydrous aluminum bromide and cobalt bromide were prepared from the corresponding Cerac/Pure, Inc., reagents by slow sublimation in silica tubes under vacuum. The anhydrous materials were handled in a helium atmosphere drybox with a water vapor level <20 ppm.

The method for investigating spectrophotometrically equilibria of the type of reaction 1 has been described elsewhere.^{1,2} A Cary Model 17H spectrophotometer equipped with a high-temperature cell compartment has been used. The optical cells were fused-silica UV type cylindrical cells (5- or 10-cm path length) purchased from Pyrocell.

The apparent molar absorptivity, ϵ , of the gaseous complex(es) and the partial pressures, P_c , of the complex(es) were determined by two different sets of experiments using Beer's law

$$\epsilon = AV/nl \quad P_c = ART/le \quad (2)$$

where A is the optical density; V , the cell volume; n , the moles of $\text{Co}(\text{II})$ in the gas phase; and l , the path length. The temperature gradient along the optical cell was adjusted so that the cell windows were 2–3 °C hotter than the center of the cell where the excess solid CoBr_2 was maintained at temperature T . Measurements of A (or P_c) as a function of time showed that equilibrium was reached in less than 30 min.

The apparent pressures, P' , of the Al_2Br_6 dimer were calculated from the amounts of Al_2Br_6 placed in the cell and the relation

$$P' = P_0 - P_D \quad (3)$$

Here P_0 is the "ideal gas" pressure of Al_2Br_6 calculated from the added

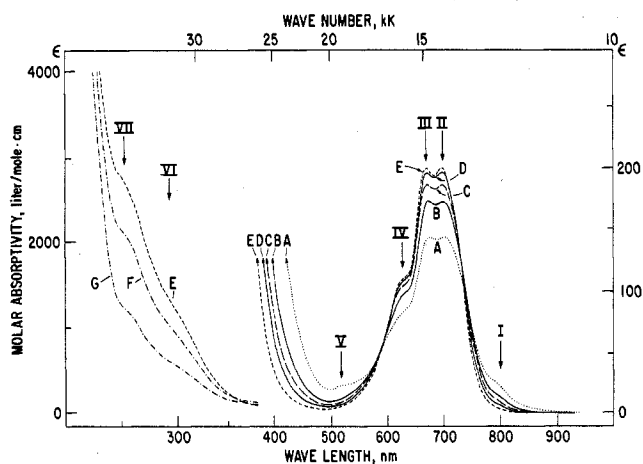


Figure 1. Absorption spectra of the cobalt bromide-aluminum bromide vapor complex(es) as a function of temperature: A, 900 K; B, 800 K; C, 750 K; D, 700 K; E, 650 K; F, 600 K; G, 550 K ($10 \text{ kK} = 1 \mu\text{m}^{-1}$).

Al_2Br_6 moles in the cell and P_D is the correction for dissociation



$$k = (2P_D)^2/P' \quad (4b)$$

The temperature dependency of the equilibrium constant, k , for reaction 4a was derived from the JANAF tables⁹

$$\ln k = 15.341 - 11598/T - 497106/T^2 \quad (5)$$

and the derived values of k were used to calculate P_D in eq 4b. At temperatures up to 1000 K, no reaction of Al_2Br_6 with the silica container was observed.

The nature of the solid phase in equilibrium with the gases was investigated by simple experiments similar to those described previously.^{1,2} It was found that, at temperatures between 550 and 900 K and at Al_2Br_6 pressures of less than 2 atm, the only solid phase present in the cells was CoBr_2 . Furthermore, we have determined by differential thermal analysis (DTA) that presublimed CoBr_2 solid exhibits a phase transformation at $648 \pm 3 \text{ K}$. This transformation was found previously¹⁰ and attributed to changes of CoBr_2 from a low-temperature form ($P\bar{3}m1$; $\text{Cd}(\text{OH})_2$ type) to a high-temperature form ($R\bar{3}m$; CdCl_2 type). At higher temperatures, our DTA curves show that solid CoBr_2 starts to decompose at temperatures near 875 K. Melting and simultaneous partial decomposition occur in the range 927–1000 K. From a broad melting DTA curve, the melting point was estimated to be $\sim 953 \pm 10 \text{ K}$.

Results and Discussion

Molar Absorptivity and Electronic Spectra. Four experiments were conducted to determine the molar absorptivity of the gaseous complex(es) at different pressures of Al_2Br_6 and different temperatures. Table I¹¹ shows that within experimental error the absorptivity is independent of the Al_2Br_6 pressure. This implies either that one gaseous species is present or that two or more species with equal "atomic absorptivities" are present. The temperature dependence of the spectrum is shown in Figure 1. The maximum molar absorptivity at $1.435 \mu\text{m}^{-1}$ can be represented as a function of temperature within $\pm 5\%$ by the equation

$$\epsilon_{\text{max}} = -46.38 + 0.853T - 7.252 \times 10^{-4}T^2 \quad (6)$$

$550 \leq T \leq 900 \text{ K}$

The absorption spectra of the complex(es) in the 1.0 – 5.0 - μm^{-1} region are characterized by a broad set of d-d bands in the region 1.2 – $2.0 \mu\text{m}^{-1}$ and a tail of a high-intensity charge-transfer band having two shoulder bands, one at $\sim 3.3 \mu\text{m}^{-1}$ and the other at $3.77 \mu\text{m}^{-1}$. Apart from a red shift, the d-d spectra of the bromoaluminate complex(es) are very similar to the corresponding chloroaluminate complexes.³ There are

two strong bands, II and III (at 1.43 and $1.49 \mu\text{m}^{-1}$), a medium-intensity band, IV (at $\sim 1.6 \mu\text{m}^{-1}$), and two weak bands, I and V (at 1.25 and $1.95 \mu\text{m}^{-1}$). These bands probably arise, as in the case of the CoAl_2Cl_8 , from the ${}^4A_{2g}(\text{F}) \rightarrow {}^4T_{1g}(\text{F})$ and ${}^4T_{1g}(\text{P}) \rightarrow {}^4T_{1g}(\text{F})$ transitions of the $d^7 \text{Co}(\text{II})$ configuration in a near-octahedral bromide field and/or the fine-structure interactions³ of the ${}^4T_{1g}(\text{P}) \rightarrow {}^4A_{2g}(\text{F})$ transition in a tetrahedral CoBr_4^{2-} field. The absorption spectra of CoBr_4^{2-} in CH_3CN solution¹² also show bands II–IV with maximum absorptivities of ~ 1000 , 700 , and $250 \text{ M}^{-1} \text{ cm}^{-1}$, respectively. In addition, the solution spectra show a band with $\sim 1100 \text{ M}^{-1} \text{ cm}^{-1}$ absorptivity at $\sim 1.37 \mu\text{m}^{-1}$. For octahedral CoBr_6^{4-} , as in the case of other octahedral first-row transition metal complexes, an absorptivity much less than $100 \text{ M}^{-1} \text{ cm}^{-1}$ is expected at this wavenumber range. The temperature dependence of the spectra shown in Figure 1 is similar to that measured and theoretically predicted for the tetrahedral $(\text{Bu}_4\text{N})_2\text{CoBr}_4$ complex¹³ and thus supports a tetrahedrally coordinated $\text{Co}(\text{II})$ in the gas phase. However, the intermediate values of the molar absorptivity suggest a scheme¹⁴ in which both octahedral (O) and tetrahedral (T) cobalt species are present in equilibrium



Assuming, for example, a molar absorptivity $\epsilon_T \sim 1000 \text{ M}^{-1} \text{ cm}^{-1}$ for the tetrahedral species and a value $0 < \epsilon_O < 50 \text{ M}^{-1} \text{ cm}^{-1}$ for the molar absorptivity of the octahedral species, then from the equation

$$\epsilon = (1-x)\epsilon_T + x\epsilon_O \quad (8)$$

and from the observed value $\epsilon \sim 200$ at 650 K , we can estimate the mole fraction, x , of the octahedral cobalt to be in the range $0.8 < x < 0.84$. Temperature variations will change¹³ the ϵ_T values and simultaneously affect the equilibrium constant of reaction 7, yielding different x values. Thus, in principle, the relative changes with temperature of $\epsilon(\text{observed})$ and $\epsilon_T(\text{predicted})$ ¹³ could be used to calculate the thermodynamics of reaction 7. However, the values for the temperature coefficients of the observed ϵ (Figure 1) and the ϵ_T of $(\text{Bu}_4\text{N})_2\text{CoBr}_4$ are similar and do not permit, within experimental errors, such thermodynamic calculations.

In the previous study³ of the CoCl_2 – Al_2Cl_6 system, it was argued that equilibrium 7 shifts to the right with increasing temperature. In view of the above discussion, such a shift would be possible *only* if ϵ is decreased *faster* than ϵ_T with increasing temperature. The relative values of ϵ_T and ϵ , however, cannot be determined experimentally, and thus the argued temperature shift³ of eq 7 cannot be considered conclusive. For both the CoCl_2 and CoBr_2 systems with aluminum halides, we believe that the intermediate values of the molar absorptivity indicate a partition of the $\text{Co}(\text{II})$ gaseous species into two coordinations, one close to octahedral and one close to tetrahedral, the octahedral being the predominant species. The temperature dependence of the spectra is mainly attributed to changes of the absorptivity of the tetrahedral species, ϵ_T , with temperature. As we will discuss later, the presence of octahedrally coordinated $\text{Co}(\text{II})$ as the main species is also supported by thermodynamic considerations (see the discussion relevant to Table III).

Finally, we should like to note that the two shoulder charge-transfer bands, VI and VII, in Figure 1 are very close in frequency to the bands observed for CoCl_4^{2-} at ~ 3.5 and $3.72 \mu\text{m}^{-1}$ ¹⁵ and are assigned $\pi t_1 \rightarrow dt_2$ CT electronic transitions.

Partial Pressures and Thermodynamics. Nine spectrophotometric experiments with different pressures, P' , of Al_2Br_6 over excess solid CoBr_2 were performed yielding the values of A_{max} and partial pressures, P_c , given in Table II.¹¹ Figure 2 shows that the pressure of the gaseous complex(es), P_c , is

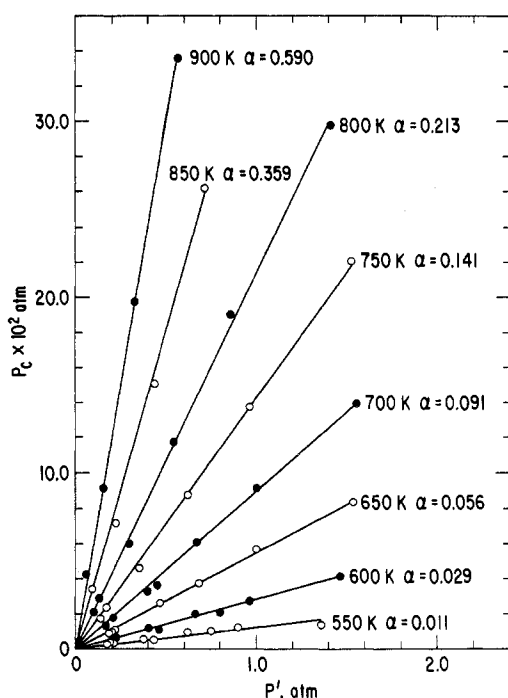


Figure 2. Plots of P_c vs. P' at different temperatures. The slopes α were determined from a least-squares treatment of the data.

proportional to the pressure of the Al_2Br_6 dimer

$$P_c = \alpha_T P' \quad (9)$$

This implies^{1,2} that each gaseous species was formed with one Al_2Br_6 molecule per mole. Thus, in eq 1, the value of n is 1 and the general formula of the gaseous complex(es) is $(\text{CoBr}_2)_m \text{Al}_2\text{Br}_6$ ($m = 1, 2, \dots$). The "atomic absorptivities" of complexes having different numbers of Co(II) atoms are expected to be different, and thus the requirement imposed by the pressure-independent molar absorptivity (see above) implies that a single gaseous complex with $m = 1$ or 2 (or more) predominates. However, we consider it reasonable to assume that the predominant gaseous complex is mononuclear in Co(II) (i.e., $m = 1$). This assumption has been used previously for the chloroaluminate complexes¹⁻⁸ and is based on the observation that all known solid complexes of transition metal halides with aluminum halides always contain one transition metal ion per mole of complex. Thus, the stoichiometry of the predominant gaseous complex is believed to be CoAl_2Br_8 . However, since thermodynamic considerations cannot distinguish between molecules having the same stoichiometry but different structures, it is possible that two or more species with the same stoichiometry CoAl_2Br_8 but different Co(II) coordinations are present and contribute in the light absorption.

With the values $n = m = 1$, the equilibrium constant of eq 1 was calculated (Table II) from the moles, M_0 , of Al_2Br_6 introduced into the cell, from the mole balance equation, $M_0 = M_{\text{Al}_2\text{Br}_6} + 2M_{\text{AlBr}_3} + M_{\text{CoAl}_2\text{Br}_8}$, and by use of eq 2 and 3. The values of $R \ln K$ vs. $1/T$ are plotted in Figure 3. The arrows in the figure indicate the temperatures found by our DTA measurements at which the crystal transformation and decomposition of CoBr_2 occur. The enthalpy and entropy of the crystal transformation have been estimated¹⁰ to be $\Delta H < 100$ cal/mol and $\Delta S < 0.15$ eu; thus, within our experimental accuracy, the existence of the two crystalline forms of CoBr_2 will not alter the measured thermodynamic quantities of reaction 1. A reduction of the apparent enthalpy and entropy according to the second law can be deduced from Figure 3. The least-squares treatment of the data at temperatures below

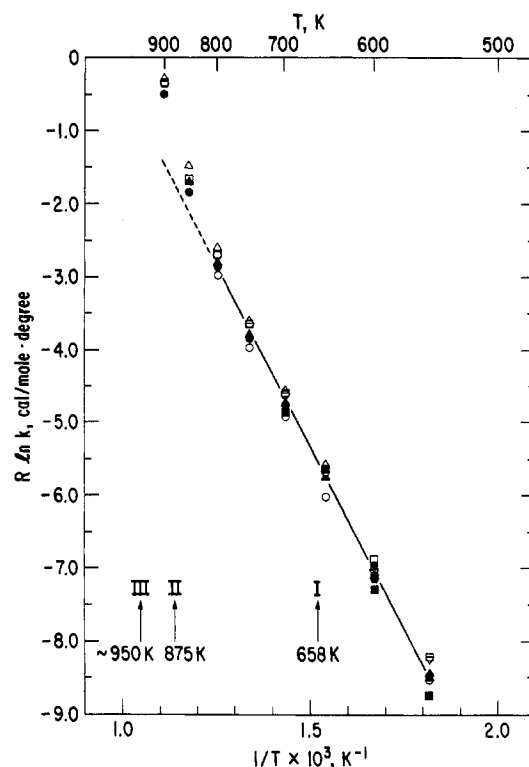


Figure 3. Plot of $R \ln K$ (cal/(mol deg)) vs. $1/T$ for reaction A in Table III: I, crystal transformation; II, decomposition range of CoBr_2 ; III, approximate melting point of CoBr_2 ; ∇ , E-3; \circ , E-4; \bullet , E-5; \blacktriangle , E-6; Δ , E-7; \blacksquare , E-8; \square , E-9; \bullet , E-10; \circ , E-11.

Table III. Thermodynamic Quantities for Solid-Gas Reactions

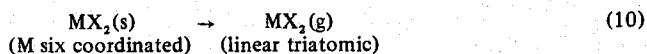
| Reaction | ΔH^a , kcal/mol | ΔS^a , eu | Temp range, K | Ref |
|---|-------------------------|-------------------|---------------|-----------|
| (A) $\text{CoBr}_2(\text{s}) + \text{Al}_2\text{Br}_6(\text{g}) \rightarrow \text{CoAl}_2\text{Br}_8(\text{g})$ | 9.9 ± 0.13 | 9.4 ± 0.2 | 550-800 | This work |
| (B) $\text{CoCl}_2(\text{s}) + \text{Al}_2\text{Cl}_6(\text{g}) \rightarrow \text{CoAl}_2\text{Cl}_8(\text{g})$ | 10.0 ± 0.2 | 9.8 ± 0.3 | 600-800 | 3 |

^a Determined from the relation $RT \ln K = T\Delta S - \Delta H$, assuming ΔS and ΔH are constant over the entire temperature range.

the decomposition region of CoBr_2 yielded the values listed in Table III. The points at 850 K and especially the points at 900 K deviate from the straight line (Figure 3) established by all other points at lower temperatures (800-550 K) with a minimum statistical error. These deviations might be attributed to the partial decomposition of CoBr_2 and its effect on the calculations of both the molar absorptivity and the partial pressure of complex. For the molar absorptivity experiments, partial decomposition of CoBr_2 will decrease the amount of CoBr_2 carried in the gas phase and lower the values of the measured absorbance. Thus, lower ϵ , higher P_c , and higher K values will be calculated. For example, if we assume that a 10% decomposition of CoBr_2 takes place at 900 K in the cells used for the determination of molar absorptivity, then we could calculate a new value of ϵ , approximately 18% higher than the value reported in Table I. Such an increase will in turn decrease the values of the equilibrium constant of reaction 1 by $\sim 25\%$ and bring the 900-K points in Figure 3 closer to the straight line.

The values of the thermodynamic quantities for the $\text{CoBr}_2\text{-Al}_2\text{Br}_6$ reaction are, within experimental error, the same as the values listed in Table III for the corresponding $\text{CoCl}_2\text{-Al}_2\text{Cl}_6$ reaction. This is best interpreted as implying that the bonding of the Co(II) in the gaseous complex is very similar to that in the solid. A literature survey^{9,16} of the heats of sublimation of MX_2 ($M = \text{Mg, Cr, Mn, Fe, Co, Zn}$) solids

having a layer-type (CdCl_2) structure shows that the sublimation process



is 6–10 kcal/mol more endothermic for the chloride salts than for the bromide salts. Reaction 10 is associated with the destruction of four M–X bonds; thus, if reactions A and B in Table III were associated with the destruction of two (or more) cobalt–halide bonds, we would expect a difference of at least 2–3 kcal/mol between their enthalpies of formation. Since the enthalpies are nearly the same, it appears likely that the $\text{Co}^{\text{II}}\text{-X}$ in both gaseous complexes might have a very similar coordination to that in the solid, i.e., a sixfold coordination. These findings support our previous conclusions and indicate that in the predominant gaseous complex, the $\text{Co}(\text{II})$ is in a close-to-octahedral coordination. This is at variance with the interpretations of Anundskås et al.⁵ and of Emmenegger,⁴ who infer a tetrahedral coordination.

Volatility Enhancement Ratios. From a practical point of view, it should be useful to calculate and compare the volatility enhancement ratios $R(T)$ of the cobalt halides in different environments of “acidic gases”. For the general reaction 1

$$R(T) = P_c(T)/P_s(T) \quad (11)$$

where $P_s(T)$ is the vapor pressure of solid MX_2 and $P_c(T)$, the partial pressure of the complex. In terms of the thermodynamic quantities of reaction 1, we have

$$R(T) = \frac{P'}{P_s(1 + K^{-1})} = \frac{P'}{P_s} \left(1 + e^{\Delta H/RT - \Delta S/R} \right)^{-1} \quad (12)$$

Equation 12 shows that increasing the temperature and/or pressure of Al_2X_6 increases the volatility enhancement ratio. Also, because of dissociation (4), the pressure of the dimer depends on the equilibrium constant k (eq 4b)

$$P' = P_0 + (k/8) \left[1 - (16P_0/k + 1)^{1/2} \right] \quad (13)$$

Combining eq 12 and 13 and taking into account the consumption of Al_2X_6 due to reaction 1, we have calculated¹⁷ and plotted in Figure 4 the temperature dependence of P_c and the logarithm of $R(T)$ for the cobalt halides in Al_2Cl_6 , Al_2Br_6 , Ga_2Cl_6 , and Fe_2Cl_6 atmospheres. A constant pressure, $P_0 = 1$ atm, was used at all temperatures. Clearly, P_c passes through a maximum which depends on the thermodynamic quantities of both reactions 1 and 4. Calculations of P_c at different P_0 pressures were made and show that with increasing pressure maximum P_c increases sharply and its position shifts to higher temperatures. The $\ln [R(T)]$ plots in Figure 4 indicate that at lower temperatures Al_2Br_6 is a better gas-complexing agent than Al_2Cl_6 for the respective cobalt halides. At higher temperatures, however, the enhancement due to the aluminum chloride is greater than that due to aluminum bromide. Iron(III) chloride appears to be superior to both at higher temperatures, but the calculated values of $R(T)$ do not include a correction for the dissociation reaction $\text{FeCl}_3 \rightleftharpoons \text{FeCl}_2 + 1/2\text{Cl}_2$; thus, the resultant curve is correct only in the presence of an overpressure of Cl_2 .

Finally, it is interesting to note that the low reactivity of Al_2Br_6 with fused silica at temperatures up to 1000 K and its high $R(T)$ values make it attractive for detailed spectrophotometric studies of gaseous complexes. Furthermore, the critical constants $T_{\text{crit}} = 763$ K and $P_{\text{crit}} = 28.5$ atm⁹ of Al_2Br_6 permit pressures of nearly 30 atm at temperatures near 800 K, where there is practically no attack on fused silica. Under these conditions, aluminum bromide can be considered as a potential candidate for the construction of gas lasers by

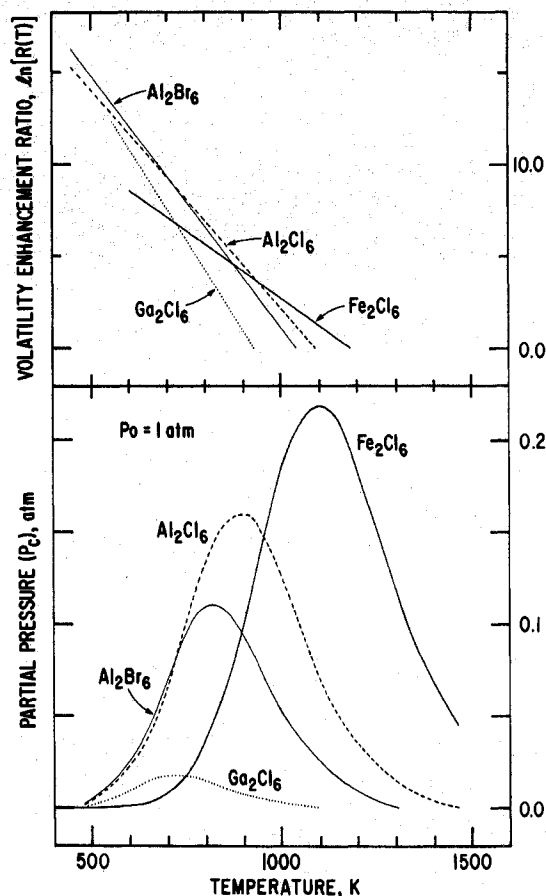


Figure 4. Apparent partial pressures and volatility enhancement ratios of CoCl_2 and CoBr_2 in different A_2X_6 atmospheres. At each temperature, the “ideal gas” pressure of Al_2Cl_6 was $P_0 = 1$ atm.

complexing and carrying in the gas phase considerable amounts of lanthanide bromides. Presently, we are developing in this laboratory experimental techniques to study spectrophotometrically such bromide gas complexes at elevated pressures and temperatures.

Acknowledgment. This work was performed under the auspices of the U.S. Energy Research and Development Administration. We thank Jack Settle for help with the DTA experiments and Milton Blander for comments on the manuscript; many thanks are also expressed to Joe Royal and Janet Steinquist.

Registry No. CoAl_2Br_6 , 60873-91-8; CoBr_2 , 7789-43-7; Al_2Br_6 , 18898-34-5.

Supplementary Material Available: Table I, showing maximum absorptivities, and Table II, showing maximum absorbances, partial pressures, and equilibrium constants (3 pages). Ordering information is given on any current masthead page.

References and Notes

- G. N. Papatheodorou, *J. Phys. Chem.*, **77**, 472 (1973).
- G. N. Papatheodorou, *Inorg. Chem.*, **12**, 1899 (1973).
- G. N. Papatheodorou, *Z. Anorg. Allg. Chem.*, **411**, 153 (1975).
- A. Dell'Anna and T. P. Emmenegger, *Helv. Chim. Acta*, **58**, 1145 (1975).
- (a) A. Anundskås and H. A. Øye, *J. Inorg. Nucl. Chem.*, **37**, 1609 (1975); (b) A. Anundskås, A. E. Mahgoub, and H. A. Øye, *Acta Chem. Scand., Ser. A*, **30**, 193 (1976).
- Von Meinhard and H. Schäfer, *Z. Anorg. Allg. Chem.*, **408**, 37 (1974).
- D. M. Gruen and R. L. McBeth, *Inorg. Chem.*, **8**, 2625 (1969).
- H. A. Øye and D. M. Gruen, *J. Am. Chem. Soc.*, **91**, 2229 (1969).
- “JANAF Thermochemical Tables”, The Dow Chemical Co., Midland, Mich.
- T. J. Wydeven and N. W. Gregory, *J. Phys. Chem.*, **68**, 3249 (1964).
- Supplementary material.
- G. Chottord and J. Bolard, *Chem. Phys. Lett.*, **33**, 309 (1975).
- R. Gale, R. E. Godfrey, and S. F. Mason, *Chem. Phys. Lett.*, **38**, 441 (1976).

- (14) A. Barkott and C. A. Angell, *J. Phys. Chem.*, **79**, 2192 (1975).
 (15) B. D. Bird and P. Day, *J. Chem. Phys.*, **49**, 392 (1968).
 (16) (a) O. Kubaschewski, E. Evans, and C. B. Alcock, "Metallurgical Thermochemistry", Pergamon, 1967; (b) *Natl. Bur. Stand. (U.S.), Tech. Note*, No. 270 (1-7) (1965-1973); (c) C. E. Wicks and F. E. Black,

- U.S., Bur. Mines, Bull.*, No. 605 (1973).
 (17) The calculations were based on thermodynamic data reported in the following references: (a) $\text{Al}_2\text{Cl}_6\text{-CoCl}_2$, ref 3; (b) $\text{Al}_2\text{Br}_6\text{-CoBr}_2$, this work; (c) $\text{Ga}_2\text{Cl}_6\text{-CoCl}_2$, ref 5; (d) $\text{Fe}_2\text{Cl}_6\text{-CoCl}_2$, E. W. Dewing, *Mettall. Trans.*, **1**, 2169 (1970).

Contribution from the Department of Chemistry,
 University of Wyoming, Laramie, Wyoming 82071

Physical Properties of Linear-Chain Systems. 7. Magnon Sidebands in the Electronic Absorption Spectra of CsCoCl_3 and RbCoCl_3 ¹

CHARLES F. PUTNIK and SMITH L. HOLT²

Received November 1, 1976

AIC607783

The polarized, single-crystal absorption spectra of the linear-chain materials CsCoCl_3 and RbCoCl_3 have been measured at several temperatures between 298 and 4.2 K. Spectral analysis reveals a surprising number of magnon sidebands which have been carefully examined. The sidebands are found to persist to temperatures well above the three-dimensional, antiferromagnetic ordering temperature of the materials. The thermal behavior of the sidebands exhibits a strong correlation with the results obtained from magnetic susceptibility and neutron diffraction measurements. The results indicate that long-range spin correlation exists in one dimension over a wide span of temperature above the Neél point. It appears that this region of one-dimensional spin correlation is a quasi-intermediate phase between three-dimensional magnetic order and paramagnetism in these compounds. The results also expose new facets relating to the mechanism of sideband absorption with which theory may be refined.

Introduction

There are now a number of examples of intensity enhancement of formally spin-forbidden ($\Delta S \neq 0$) electronic transitions in magnetically concentrated systems.³ Mechanisms have been postulated for the relaxation of the $\Delta S = 0$ spin selection rule and theoretical predictions of the temperature dependence of the exchange-enhanced oscillator strengths have been offered.⁴⁻¹⁷ In an effort to ascertain whether the proposed mechanisms are applicable to systems in which the exchange interactions are predominantly one-dimensional, we have investigated a series of compounds of the formulation ABX_3 . This class of compounds includes materials where B is any divalent, first-row transition metal ion; A is Rb^+ , Cs^+ , or any of several alkylammonium cations; and X is either Cl^- , Br^- , or I^- .¹⁸ All compounds of interest crystallize in a hexagonal cell with linear chains of face-sharing $[\text{BX}_6]^{4-}$ octahedra extending along the *c* crystallographic axis. The A cations occupy sites between adjacent chains and the resulting separation provides an effective interchain "magnetic insulation".

Our optical investigations of materials of this type have centered upon the compounds ANiX_3 [$\text{A}^+ = (\text{CH}_3)_4\text{N}^+$, Rb^+ , Cs^+ ; $\text{X}^- = \text{Cl}^-$, Br^-],¹⁹ AFeX_3 [$\text{A}^+ = \text{Cs}^+$, Rb^+ ; $\text{X}^- = \text{Cl}^-$, Br^-],³ CsMnBr_3 ,²⁰ RbMnBr_3 ,²¹ $(\text{CH}_3)_4\text{NMnBr}_3$,²² and ACrCl_3 [$\text{A}^+ = \text{Rb}^+$, Cs^+].¹ In all cases we have found evidence of cooperative electronic transitions in which formal spin-selection rules are relaxed but have observed that the temperature dependence of oscillator strengths of individual "spin-forbidden" transitions within a compound and between compounds can vary markedly.

In the present work we have extended our measurements to CsCoCl_3 and RbCoCl_3 . We have recorded the behavior of exchange-assisted "spin-forbidden" transitions and have identified exciton minus magnon sidebands (magnon hot bands), exciton plus magnon sidebands (magnon cold bands), and the associated excitonic origin peaks in these one-dimensional magnetic systems.

Crystal Structures. Soling has reported the crystal structures of CsCoCl_3 ²³ and RbCoCl_3 .²⁴ Both crystallize in the space group $P6_3/mmc$ with two formula units per primitive cell. The

cell dimensions are $a = 7.2019$ (4) Å and $c = 6.0315$ (5) Å for CsCoCl_3 and $a = 6.999$ (1) Å and $c = 5.996$ (1) Å for RbCoCl_3 . These compounds are isostructural with CsNiCl_3 , the predominant structural feature being linear chains of face-sharing $[\text{CoCl}_6]^{4-}$ octahedra lying along the *c* axis.

Magnetic Properties. The transition to antiferromagnetic order in CsCoCl_3 has been determined to occur at 21.5 K from neutron diffraction measurements.²⁵ The Neél temperature of RbCoCl_3 has not been reported but in comparison to other members of this class of compounds it is expected to be some 5-10 K above that of CsCoCl_3 (e.g., for RbCoBr_3 , $T_N = 36$ K;²⁶ for CsCoBr_3 , $T_N = 28$ K;²⁷ for RbNiCl_3 , $T_N = 11$ K;²⁸ and for CsNiCl_3 , $T_N = 4.5$ K²⁸).

At 4.2 K the magnetic structure of CsCoCl_3 consists of antiferromagnetic planes stacked antiferromagnetically along the *c* axis.²⁵ Between 8 K and T_N a different magnetic structure exists which has not been characterized. A similar change occurs in the isostructural material CsCoBr_3 .²⁷ In that compound the spin structure at low temperature is essentially the same as for CsCoCl_3 but with a slight canting of the spins off the *c* axis. In the structure which exists between 14 K and T_N one-third of the chains are disordered and the other two-thirds are antiferromagnetically coupled in the basal plane.

Experimental Section

Deep blue single crystals of CsCoCl_3 and RbCoCl_3 were prepared as described previously with anhydrous CoCl_2 and the appropriate alkali chloride was used as starting material.²⁰ Preparation of thin crystals (0.020-0.025 cm) suitable for σ and π spectral measurements was facilitated by the easy cleavage of the crystals in planes parallel to the *c* crystallographic axis. The high resistance of the crystals to cleavage perpendicular to the *c* axis prevented our obtaining samples suitable for axial measurements. Our spectrometer and cryogenic system have been described earlier.²⁰

Results

The general features of the spectra of CsCoCl_3 and RbCoCl_3 are very similar and will be presented simultaneously. The spectra will be described under the general headings of the transitions between the octahedral crystal field states of the d^7 electronic configuration. More detailed analysis including